

Low-bandwidth control scheme for an oscillator stabilized Josephson qubit

R. H. Koch, J. R. Rozen, G. A. Keefe, F. M. Milliken, C. C. Tsuei, J. R. Kirtley, and D. P. DiVincenzo

IBM Watson Research Ctr., Yorktown Heights, NY 10598 USA

(Dated: June 26, 2018)

We introduce a new Josephson junction circuit for which quantum operations are realized by low-bandwidth, nearly adiabatic magnetic-flux pulses. Coupling to the fundamental mode of a superconducting transmission line permits a stabilization of the rotation angle of the quantum operation against flux noise. A complete scheme for one-qubit rotations, and high-visibility Ramsey-fringe oscillations, is given. We show that high visibility depends on passing through a portal in the space of applied fluxes, where the width of the portal is proportional to the ramp-up rate of the flux pulse.

Among the many candidates for the physical implementation of a quantum computer, Josephson junction circuits have always been among the most promising. The quantum behavior of these circuits is readily tailorable by the choice of electrical topology and circuit parameters: there are various regions of this parameter space in which a coherent, controllable two-level quantum system, suitable for the realization of a qubit, is possible. This same tailorability must also be exploited to avoid strong coupling to the environment and other decohering effects. The complexity of this optimization[1] is such that many distinct Josephson circuit qubits are under active study, with successful single qubit control and two-qubit coupling achieved in a number of cases[2, 3]. But further improvements in qubit performance are unquestionably needed and continue to be sought. Recently, another important degree of freedom has been added to this search: strong, coherent coupling between a Josephson junction qubit and a quantized harmonic oscillator, realized by a superconducting transmission line, has been achieved[4, 5]. This exciting discovery raises the question of how best such a coupled system is to be exploited for quantum information processing.

In this Letter we report a new class of Josephson flux qubits that enter novel regions of the design space to achieve superior qubit performance. Here are its features: First, our qubit can be placed in a “frozen” state in which the barrier is very high, which makes resetting and measuring the qubit very reliable. Second, and more important, all qubit operations are realized by low-bandwidth, nearly adiabatic operations. Since the amount of environmental noise seen by the qubit is proportional to this bandwidth, we gain significantly by requiring only an approximately 1 GHz control bandwidth rather than the many GHz that are necessary in other control schemes, which require the transmission of microwave radiation to the qubit. Finally, within our adiabatic operation scheme, the presence of a coupled quantum harmonic oscillator plays a specific role in the qubit operation: the qubit rotation angle, which is equal to the dynamical phase difference accumulated between ground and excited state energy surfaces, is stabilized by the adiabatic conversion of the qubit states to the ground and excited

states of the quantum oscillator.

The resulting qubit with its associated control transmission lines is complex, but the advantages gained by our operation strategy leads to a qubit for which a scale up to larger systems will eventually be more feasible. Our experimental realization of this qubit system is shown in Fig. 1. The device consists of three Al/Al₂O₃/Al Josephson junctions grown using an in-house shadow mask process, arranged in a gradiometer pattern. This design is a modification of a qubit previously reported[6]. The body of the gradiometer is aluminum and consists of three loops. The lower loop is threaded by external flux Φ , the small left loop is threaded by the flux Φ_C ; the upper loop, the “pickup” loop, is inductively coupled to a high-Q niobium superconducting microstrip “pickup” transmission line. There are no wires attached to the qubit. Readout is done using a dc SQUID inductively coupled to the pickup transmission line. The qubit is operated at 30 mK; however the effective electrical temperature from the circuits that drive the fluxes Φ and Φ_C is about 1.3 K. These circuits are not shown; however, these are coupled to the qubit with two additional superconducting microstrip transmission lines. The lines are shorted at the end that is not connected to the room temperature electronics. The length of the lines between the qubit and the shorted ends are such that at the desired frequency of operation of the qubit, 1.54 GHz, there will be a current node at the location of the qubit. Hence, when we operate the qubit at the degenerate point, which we can tune to have an operating frequency of 1.54 GHz, the contributions from both the low-frequency noise and the noise at the operating frequency are minimized.

Using our network graph theory[6], we have obtained a comprehensive quantum mechanical model for this qubit. The system Hamiltonian is equivalent to that of a massive particle in a four-dimensional potential. The particle mass is set by the system capacitances; the four degrees of freedom are the three Josephson junction phases plus the phase (the time integral of a voltage) across the capacitance of the transmission line LC resonance. Other environmental degrees of freedom, e.g., those associated with the control transmission lines, are modelled as in [6] using an oscillator bath. We calculate that the in-

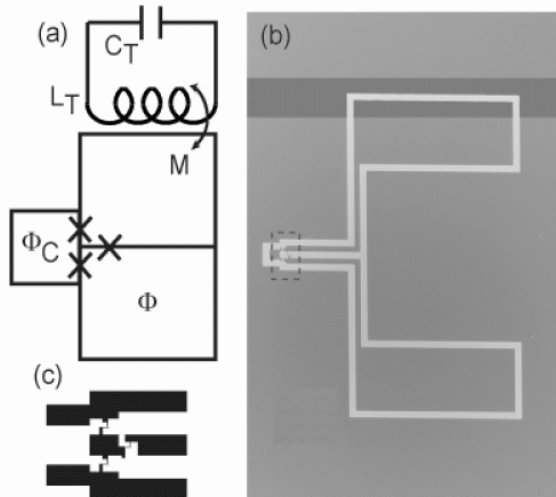


FIG. 1: (a): Schematic layout of the qubit and the harmonic oscillator equivalent of the transmission line. (b): Picture of the qubit. The qubit is $500 \mu\text{m}$ long and each junction is 250 by 250 nm^2 in size. On the upper loop the pickup transmission line is shown. (c): Mask art of the three shadow type Josephson junctions (blow up of dashed box in (b)).

intrinsic quantum lifetimes associated with this bath, for the choices of control parameters described below, and for $T = 100 \text{ mK}$, are $T_2 = 600 \text{ nsec}$ and $T_1 = 300 \text{ nsec}$, which are more than long enough for our adiabatic control scheme to successfully execute quantum operations. In practice the coherence of our qubit is further decreased by extrinsic noise in the control electronics, an example of which will be analyzed below.

While the resulting potential function is complex, there is a region of two-dimensional parameter space of applied fluxes Φ and Φ_C (see Fig. 1) in which the potential has a simple, double-well structure. The lowest energy states of this double well form the qubit; the qubit is also linearly coupled to the transmission line harmonic oscillator, as we will describe shortly.

In the vicinity of these double-well minima, the three degrees of freedom of the qubit can be linearly transformed into two “fast” degrees of freedom transverse to the double-well axis and one slow longitudinal phase which we will call δ . Using a Born-Oppenheimer approximation[7] for the fast degrees of freedom, we have numerically obtained an effective one-dimensional double-well potential $V_Q(\delta)$ for the qubit. While we use the full numerical form in our calculations, it is useful for describing features of this potential to represent it using the following simple analytic anharmonic form[8]:

$$V_Q(\delta, t) = -h_2(t)\delta^2 + h_4\delta^4 + a(t)\delta. \quad (1)$$

We indicate here an explicit dependence on time t , as our qubit control technique involves the pulsing of Φ and

Φ_C in time. In our devices, to good approximation, Φ controls the double-well asymmetry coefficient a and Φ_C varies the double-well barrier height h_2 . We find that h_2 can be either positive or negative; that is, the double-well structure can be transformed into a single well.

Eq. (1) is only one part of the description of the system; coupling to the harmonic-oscillator phase φ must also be included. To good approximation, the full Hamiltonian of the system can be written

$$H = \frac{e^2 Q^2}{2C_Q} + V_Q(\delta, t) + \frac{e^2 q^2}{2C_T} + \left(\frac{\Phi_0}{2\pi}\right)^2 \frac{\varphi^2}{L_T} + \left(\frac{\Phi_0}{2\pi}\right)^2 \frac{M \delta \cdot \varphi}{L_Q L_T}. \quad (2)$$

Here the first two terms are the qubit Hamiltonian, the next two terms are the harmonic oscillator Hamiltonian, and the last term is the linear coupling between the two. Q and q , the qubit and oscillator charge operators, act as momentum operators in the Schrodinger equation: $[\varphi, q] = [\delta, Q] = i$. C_Q is the capacitance associated with the Josephson junctions; in our circuit all three have $C_Q \approx 50 \text{ fF}$ (there is substantial excess capacitance in parallel with the intrinsic capacitance of the oxide junctions). $C_T \approx 1 \text{ fF}$ and $L_T \approx 10 \text{ nH}$ are the effective transmission line capacitance and inductance, $L_Q \approx 640 \text{ pH}$ is an effective qubit inductance (actually a complicated function of the full inductance matrix of the qubit circuit[6]), $M \approx 50 \text{ pH}$ is the mutual inductance between the qubit and the transmission line, and $\Phi_0 = h/2e$ is the superconducting flux quantum. In other studies[4] the physics of this situation has been described using a Jaynes-Cummings Hamiltonian; we find that retaining the first-quantized form of Eq. (2) has proved helpful in analyzing the details of our control scheme.

In our device, the barrier height h_2 in the model potential Eq. (1), at low values of the control flux Φ_C , can easily be made so high that the quantum tunnelling rate Δ can be made very small (\hbar/Δ being many minutes at least). In this regime the qubit state is essentially frozen, with two degenerate eigenstates $|L\rangle$ and $|R\rangle$ for “left” and “right” well, see Fig. 3, point A. The device is hysteretic in this regime, so it can be stably set in either $|L\rangle$ or $|R\rangle$ by a suitable quasistatic sweeping of flux Φ . In addition, the state is easily read out by a sensing SQUID inductively coupled to the transmission line of Fig. 1.

So, for $\Phi_C = \Phi = 0$, corresponding to $a, \Delta \approx 0$, the qubit is in a “resting condition” in which its dynamics are frozen. Starting from this resting condition, conceptually there is a simple prescription for adiabatically applying single-qubit quantum gates to the qubit. A “Z rotation” (of the Bloch sphere defined by the $|L, R\rangle$ basis) is simply obtained by adiabatically varying a in Eq. (1) (by pulsing the main-loop flux Φ) with Δ held equal to zero. In the adiabatic limit, the Z rotation angle is given by $\phi = 2 \int dt \epsilon(t)/\hbar$, where $2\epsilon \equiv (\langle L|V_Q|L\rangle - \langle R|V_Q|R\rangle)$ is the

difference in depths of the two wells of V_Q .

The “ X rotation” scheme will require more discussion, as it involves a stabilizing effect due to the harmonic oscillator degree of freedom in Eq. (2). If, starting from the resting state, the control flux Φ_C is pulsed, then the ϵ defined in the last paragraph will remain zero and h_2 will be varied. Since ideally the double-well potential Eq. (1) is symmetric throughout this pulse, the lowest-lying eigenstates of this potential will always be symmetric ($|S\rangle$) and antisymmetric ($|A\rangle$) with respect to the qubit coordinate δ . In the resting state $|S, A\rangle = (|L\rangle \pm |R\rangle)/\sqrt{2}$; these basis states lie at right angles to the $|L, R\rangle$ states on the Bloch sphere, so that adiabatic evolution along this coordinate and back results in an X rotation by angle $\theta = \int dt \Delta(t)/\hbar$, where $\Delta(t) = E_1(\Phi_C(t)) - E_0(\Phi_C(t))$, and $E_{0,1}$ are the first two instantaneous eigenenergies (see Fig. 2) of the qubit Hamiltonian Eq. (2).

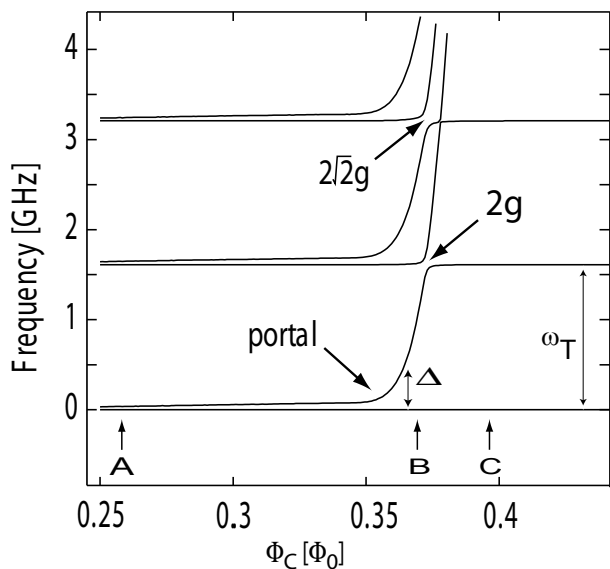


FIG. 2: Instantaneous eigenvalues of H , Eq. (2), as a function of control flux Φ_C , for main flux $\Phi \approx 0$. The exponentially rising tunnel splitting Δ , and the Φ_C -independent oscillator frequency ω_T , are indicated. At A , the “resting state”, the double-well barrier is very high and the two lowest eigenstates are nearly degenerate; here the resting state is not quite symmetric, with $\epsilon \approx 15$ MHz. For this nonideal case successful quantum operation requires that the system pass through the “portal” as described in the text. At point B , beyond the portal, quantum tunneling dominates the dynamics and the system is effectively symmetric. Beyond B the qubit comes into resonance with the transmission line oscillator, with a splitting of $2g \approx 220$ MHz. At point C , the lowest lying states have purely harmonic oscillator character.

In Fig. 3 we see that the first two eigenfunctions in the potential of Eq. (2) change form in going from point A to point B , from $|L, R\rangle$ to $|S, A\rangle$. This rapid change is actually desirable for the operation of the qubit; nu-

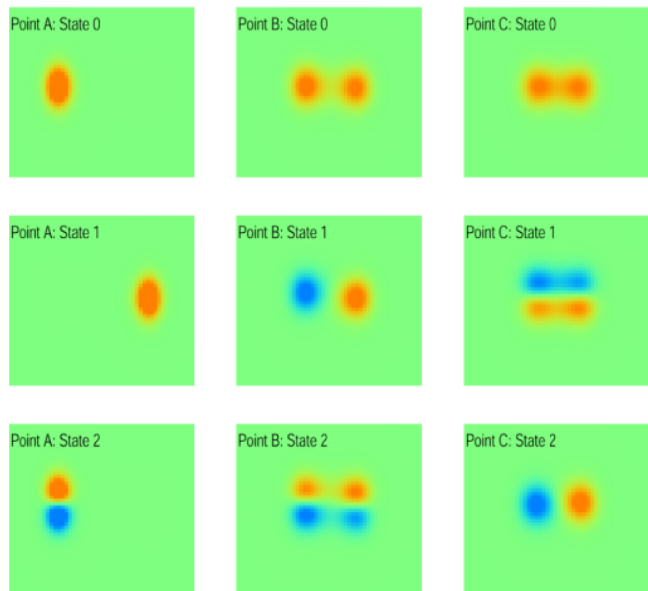


FIG. 3: Color density plot of first three first energy eigenstates of H at points A , B , and C of Fig. 2. δ is the horizontal axis, and φ the vertical axis (see Eq. (2)). For A the first two eigenstates, localized in the left and right wells, are not quite degenerate because $\epsilon \neq 0$ (see Fig. 2). In going from A to B , on account of strong quantum tunneling, the first two eigenstates change rapidly in character, becoming symmetric and antisymmetric combinations of the well states. For both A and B , the third state has one quantum of excitation of the harmonic oscillator. The states at C have purely harmonic-oscillator character. In going from A to C , the steady decrease of the well-well separation is evident.

merical integrations of the time-dependent Schrodinger equation show that we obtain high-fidelity quantum operations if $\Phi_C(t)$ is pulsed with an overall rise time of 15 nsec, with appropriate pulse shaping (see the discussion of visibility-limiting mechanisms below).

Without the coupled harmonic oscillator, this X -rotation scheme suffers from the problem that Δ , and thus θ , is exponentially sensitive to the value of Φ_C . This exponential sensitivity to the barrier height is evident in Fig. 2 for values of Φ_C near B . However, the presence of the oscillator degree of freedom changes several features of the spectrum in a dramatic way. The essentially horizontal lines in Fig. 2 are the equally spaced oscillator energy levels, which are insensitive to the flux applied to the qubit. But because of the mutual inductance M in the last term of Eq. (2), there is an avoided crossing between the oscillator and qubit eigenlevels. For the parameters of the device in Fig. 1, the “vacuum Rabi splitting” $2g$ (in the notation of the Jaynes-Cummings model, see [4]) indicated in Fig. 2 is about 220 MHz. For the 15 nsec ramp-up time mentioned above, the time-evolution remains accurately adiabatic through this anticrossing as well. Thus, after ramping up Φ_C to point C in Fig. 2,

the system remains in a superposition of just two states, the ground state and the first excited state which now has almost entirely the character of a single quantum of excitation in the harmonic oscillator. Δ in this regime is almost completely independent of Φ_C , meaning that the execution of the X rotation in this regime is almost entirely insensitive to noise in Φ_C .

While not of direct relevance to small-angle X rotations that will be desired for quantum gates, this insensitivity is very valuable for performing the analog of a Ramsey-fringe experiment to characterize this qubit[3]. The protocol for this experiment is as follows: First, prepare the system in the state $|L\rangle$, which in the ideal case ($\epsilon = 0$) is an equal superposition of the energy eigenstates $|S\rangle$ and $|A\rangle$. Second, ramp up the control flux Φ_C adiabatically, then hold it constant at a value Φ_{hold} past the anticrossing with the harmonic oscillator state (i.e., to point C in Fig. 2). After hold time T , ramp down the control flux to the resting state, then measure the qubit in the $|L, R\rangle$ basis. The measured L probability should show Larmor oscillations of the form $\cos\omega_T T$, where $\omega_T = 1/\sqrt{C_T L_T}$ [10].

We believe that the inaccuracy in the setting of the resting state, i.e., the inability to set ϵ exactly equal to zero, is likely to be the most important mechanism for reducing visibility in our system. If the resting state is not exactly symmetric, then, since Δ is exponentially small at point A , it is likely that $\Delta \ll \epsilon$. In this case $|L\rangle$ is not an equal superposition of energy eigenstates, but is an eigenstate itself, as Fig. 2a shows. Thus, a completely adiabatic evolution will keep the system at all times in an instantaneous eigenstate, and no Larmor oscillations will take place – the visibility will be zero.

The resolution to this dilemma is that, for the realistic case in which $\epsilon \neq 0$, the time evolution in the Ramsey experiment we have discussed is at a crucial moment actually *nonadiabatic*, in a way that permits the experiment to succeed as described. There is a “portal” in the ϵ - Δ parameter space, which, if passed through at a finite rate, results in a successful X rotation (Ramsey-fringe visibility near 100%). The idea is that since Δ rises exponentially, $\Delta(t) = \Delta_0 e^{t/\tau}$, there is a brief interval of time during which $\Delta(t) \approx \epsilon$; this sets the location of the portal in the parameter space. This is the critical time because here the form of the eigenstates of H changes quite rapidly from nearly $|L, R\rangle$ to very nearly $|S, A\rangle$, as Fig. 3 shows. The evolution here will be nonadiabatic if $\epsilon\tau/\hbar$ is not too large. That is, $-1 \leq \epsilon\tau/\hbar \leq 1$ approximately defines the width of the portal. If the time evolution passes through the portal, then nearly half of the state amplitude is transferred from the ground state to the excited state, resulting in essentially 100% visibility.

This picture has been confirmed in detail by numerical simulations, and also emerges from an exact solution of the two-state problem in which ϵ is time inde-

pendent and Δ increases exponentially[9]; then the exact solution of the time-dependent Schrödinger equation is proportional to $c_+(t)|L\rangle + ic_-(t)|R\rangle$, where $c_{\pm}(t) = \exp(t/2\tau)J_{\pm 1/2+i\epsilon\tau/\hbar}[\Delta_0\tau/\hbar \exp(t/\tau)]$, and $J_{\nu}(x)$ is a Bessel function. With this exact solution the visibility for finite ϵ can be calculated to be $\text{sech}^2(\pi\epsilon\tau/2\hbar)$. Our numerical simulations confirm this dependence: given the existing precision of pulsed magnetic-flux control (a few $\mu\Phi_0$), a nonzero ϵ in the MHz range will typically be present. This implies that the portal will typically be located near $\Phi_C = 0.35\Phi_0$ as in Fig. 2. We numerically find a Ramsey-fringe visibility in excess of 90% if $\Phi_C(t)$ is initially ramped rapidly through the portal (from A to B in 0.8 nsec), and then brought slowly up to its final value (from B to C in 15 nsec). The necessary time dependent flux control is demanding, but can be achieved in our lab.

We believe that our qubit and its control schemes show good promise for scalability to larger systems. The relatively large size of the main loops (Fig. 1) means that establishing strong inductive couplings between qubits is straightforward, permitting fast two-qubit gates to be done. As we have already demonstrated, its large size also makes reliable, and potentially fast, readout of the qubit state quite simple. The strong coupling to a transmission line degree of freedom permits X rotations to be done that are very insensitive to flux noise, and, as other workers have recently shown, the presence of a controllable harmonic-oscillator quantum also offers new possibilities for quantum computing architectures, including easy motion of qubits and long-distance coupling of stationary qubits. Our control schemes now considerably enrich this picture.

DPDV is supported in part by the NSA and ARDA through ARO contract numbers W911NF-04-C-0098 and DAAD19-01-C-0056. Support of DARPA contract MDA972-01-C-0052 is also acknowledged. We thank Fred Brito, Guido Burkard, Dennis Newns, and the authors of [9] for helpful discussions.

-
- [1] M. Devoret, lecture notes for Les Houches Summer School Session LXXIX, *Quantum Entanglement and Information Processing*, to be published; see also M. Devoret *et al.*, cond-mat/0411174.
 - [2] Y. Nakamura *et al.*, *Nature* **398**, 786 (1999); J. E. Mooij *et al.*, *Science* **285**, 1036 (1999); C. H. van der Wal *et al.*, *Science* **290**, 773 (2000); J. R. Friedman *et al.*, *Nature*, **406**, 43 (2000); J. M. Martinis, *Phys. Rev. Lett.* **89**, 117901 (2002); T. Yamamoto *et al.*, *Nature* **425**, 941 (2003); I. Chiorescu *et al.*, *Science* **299**, 1869 (2003).
 - [3] D. Vion *et al.*, *Science* **296**, 886 (2002).
 - [4] A. Walraff *et al.*, *Nature* **431**, 162 (2004).
 - [5] I. Chiorescu *et al.*, *Nature* **431**, 159 (2004).
 - [6] G. Burkard, R. H. Koch, and D. P. DiVincenzo, *Phys. Rev. B* **69**, 064503 (2004).

- [7] D.V. Averin and C. Bruder, Phys. Rev. Lett. **91**, 057003 (2003).
- [8] Cubic and higher order terms in δ are necessary for an accurate quantitative description of V_Q , but all the important qualitative features are captured by the simple form Eq. (2).
- [9] R. Requist, J. Schliemann, A. G. Abanov, and D. Loss, cond-mat/0409096.
- [10] Experiments on the device of Fig. 1 have shown such oscillations at the expected frequency ω_T ; at $T = 40$ nsec the visibility was measured to be approximately 60%. R. H. Koch *et al.* (unpublished).